EUROPEAN FUSION DEVELOPMENT AGREEMENT

EFDA–JET–CP(04)07-26

P. Mantica, X. Garbet , C. Angioni, E. Asp, M.de Baar, Y. Baranov, R. Budny, G. Cordey, F. Crisanti , N. Hawkes , G.M.D. Hogeweij , F. Imbeaux, E. Joffrin , N. Kirneva , E. Lazzaro , X. Litaudon, M. Mantsinen, A. Marinoni, D. McDonald , M.Nora, H. Nordman , V.Parail, F. Ryter, C. Sozzi, T. Tala, A. Thyagaraja, D. Van Eester, I. Voitsekhovitch , P. de Vries, J. Weiland, K.-D. Zastrow and JET EFDA Contributors

Progress in Understanding Heat Transport at JET

Progress in Understanding Heat Transport at JET

P. Mantica[1], X.Garbet[2], C. Angioni[3], E. Asp[2], M.de Baar[4], Y. Baranov[5], R. Budny[6], G. Cordey[5], F. Crisanti[7], N. Hawkes[5], G.M.D. Hogeweij[2], F. Imbeaux[2], E. Joffrin[2], N. Kirneva[8], E. Lazzaro[1], X. Litaudon[2], M. Mantsinen[9], A. Marinoni[10], D. McDonald[5], M.Nora[9], H. Nordman[11], V.Parail[5], F. Ryter[3], C. Sozzi[1], T. Tala[12], A. Thyagaraja[5], D. Van Eester[13], I. Voitsekhovitch[5], P. de Vries[4], J. Weiland[11], K.-D. Zastrow[5] and JET EFDA Contributors*

[1]Istituto di Fisica del Plasma CNR-EURATOM, via Cozzi 53, 20125 Milano, Italy
[2]CEA Cadarache, Association EURATOM-CEA, 13108, St Paul-Lez-Durance, France
[3]Max-Planck-Institut für Plasmaphysik, EURATOM Association, Garching, Germany
[4]FOM-Instituut voor Plasmafysica,Associatie Euratom-FOM, Nieuwegein, The Netherlands
[5]Culham Science Centre, EURATOM/UKAEA Fusion Association, Oxon. OX14 3DB, UK
[6]PPPL, Princeton University, P.O. Box 451, Princeton, NJ 08543, USA
[7]Associazione EURATOM-ENEA sulla Fusione, Via Enrico Fermi 27, 00044 Frascati, Italy
[8]RRC "Kurchatov Institute", Moscow, Russia
[9]Association EURATOM-Tekes, Helsinki Univ. of Technology, FIN-02015, TKK, Finland
[10]Dipartimento di Ingegneria Nucleare, Politecnico di Milano, Milano, Italy
[11]Association EURATOM-VR, Chalmers University of Technology, Gˆteborg, Sweden
[12]Association EURATOM-Tekes, VTT Processes, FIN-02044 VTT, Finland
[13]LPP-ERM/KMS, Association Euratom-Belgian State, TEC, B-1000 Brussels, Belgium
** See annex of J. Pamela et al, "Overview of JET Results ", (Proc.20 th IAEA Fusion Energy Conference, Vilamoura, Portugal (2004).*

Preprint of Paper to be submitted for publication in Proceedings of the
20th IAEA Conference,
(Vilamoura, Portugal 1-6 November 2004)

ABSTRACT.
This paper reports recent progress in understanding heat transport mechanisms either in conventional or advanced tokamak scenarios in JET. A key experimental tool has been the use of perturbative transport techniques, both by ICH power modulation and by edge cold pulses. The availability of such results has allowed careful comparison with theoretical modelling using 1D empirical or physics based transport models, 3D fluid turbulence simulations or gyrokinetic stability analysis. In conventional L- and H-mode plasmas the issue of temperature profile stiffness has been addressed. JET results are consistent with the concept of a critical inverse temperature gradient length above which transport is enhanced by the onset of turbulence. A threshold value R/L_{Te}~5 has been found for the onset of stiff electron transport, while the level of electron stiffness appears to vary strongly with plasma parameters, in particular with the ratio of electron and ion heating: electrons become stiffer when ions are strongly heated, resulting in larger R/L_{Ti} values. This behaviour has also been found theoretically, although quantitatively weaker than in experiments. In plasmas characterized by Internal Transport Barriers (ITB), the properties of heat transport inside the ITB layer and the ITB formation mechanisms have been investigated. The plasma current profile is found to play a major role in ITB formation. The effect of negative magnetic shear on electron and ion stabilization is demonstrated both experimentally and theoretically using turbulence codes. The role of rational magnetic surfaces in ITB triggering is well assessed experimentally, but still lacks a convincing theoretical explanation. Attempts to trigger an ITB by externally induced magnetic reconnection using saddle coils have shown that MHD islands in general do not produce a sufficient variation of ExB flow shear to lead to ITB formation. First results of perturbative transport in ITBs show that the ITB is a narrow layer with low heat diffusivity, characterized by sub-critical transport and loss of stiffness.

1. INTRODUCTION

The understanding of the physics of turbulence driven transport, although having progressed significantly in recent years [1], is nevertheless still insufficient to allow a safe extrapolation to next step plasmas to corroborate the predictions based on global scaling laws. Heat transport issues like temperature profile stiffness in ELMy H-mode or Internal Transport Barrier (ITB) formation mechanisms in Advanced Tokamak scenarios clearly have a significant impact on the expected plasma performance and therefore deserve careful attention in present-day machines in order to optimize the way of operating a next step device. This paper reports recent progress made at JET in this direction. Focussed perturbative transport experiments, both by ICRF power modulation [2] and by edge cold pulses [3], have been a key tool, together with careful comparison of these results with theoretical modelling using either empirical and semi-empirical models (critical gradient [4], Bohm-gyroBohm [5]), 1D fluid models (Weiland [6], GLF23 [7]), or 3D fluid turbulence simulations (TRB [8]: non-linear, electrostatic; CUTIE [9]: global, non-linear, electromagnetic), and in some cases gyrokinetic stability analysis (GS2 [10], KINEZERO [11]).

2. TEMPERATURE PROFILE STIFFNESS IN ELMY H-MODE PLASMAS

Stiffness of Temperature (T) profiles is predicted by the theory of electrostatic turbulence, such as the Ion/Electron Temperature Gradient (ITG/ETG) modes and the Trapped Electron Mode (TEM), as the result of an increase of transport driven by the onset of turbulence above a critical value of the inverse temperature gradient length R/L_{Tc}, which therefore cannot be much exceeded. This does not however imply an absolute rigidity of profiles over the whole plasma, the local behaviour of the temperature profile being determined by the local values of the threshold and stiffness strength, which is not necessarily high, and by the power deposition profile. The goal of the study conducted on JET and in parallel on other EU tokamaks [1, 4] was to quantify the electron stiffness using an empirical critical gradient model for the electron heat diffusivity χ_e of the form

$$\chi_i = \chi_s q^{\nu} \frac{T_e}{eB}\frac{\rho_s}{R}\left(\frac{-R\delta_r T_e}{T_e} - \kappa_s\right)\mathrm{H}\left(\frac{-R\delta_r T_e}{T_e} - \kappa_s\right) + \chi_0 q^{\nu}\frac{T_e}{eB}\frac{\rho_s}{R} \qquad (1)$$

where B is the magnetic field, q is the safety factor, $\rho_s = \sqrt{m_i T_e}/eB$, and H the Heaviside function. ν has been set =3/2 [4] from constraints by experimental data and in agreement with theoretical predictions of ITG/TEM turbulence. The 3 parameters κ_c, χ_0 and χ_s have been derived from T_e modulation experiments and their variation with plasma parameters has been compared with 1st principle models.

2.1 EXPERIMENTAL RESULTS

T_e modulation experiments have been performed in L-mode and type III ELMy H-mode plasmas at low collisionality [12,13] (B_T~3.2-3.6T, I_p~1.8MA, q_{95}~7, n_{e0}~5 $10^{19}m^{-3}$) using ICRF power in mode conversion scheme, i.e. in the presence of ^{3}He concentrations ~20% maintained via Real Time Control. This scheme allows direct and localized power deposition to electrons [2]. Up to 18MW of NBI power and 4MW of ICRH power modulated with half depth at 15-45Hz with duty cycle ~60% were applied.

The modulation and the steady-state data are simultaneously best-fitted using the model in Eq.(1). Evidence was found for the existence of a threshold in R/L_{Te}~5 for the onset of stiff transport. L- and H-modes behave in a similar way with regard to core heat transport, with similar stiffness levels and thresholds, higher central temperatures in H-mode being mainly due to the existence of an edge pedestal. The degree of profile stiffness χ_s was found to vary over a range χ_s ~1.5-6. The reason for such large variations has been identified to be the variation in ion heating power: electrons get stiffer when ion heating is increased, resulting in higher values of R/L_{Ti}. Figure.1 shows the electron heat flux properly normalized vs R/L_{Te}. Dots are steady-state data and lines are fit to modulation data. One can see that steady-state data do not allow the recognition of different degrees of stiffness (i.e. different slopes above threshold) while a weaker stiffness can be inferred from modulation data in plasmas with dominant electron heating with respect to plasmas with significant ion heating. The electron stiffness χ_s is progressively increasing with R/L_{Ti} as shown in figure 2,

and is not simply related to the value of the ratio T_e/T_i, as it was originally proposed in [13].

A comparison between the findings on profile stiffness from these experiments and the recent ITPA two-term scaling law for energy confinement has been carried out: no major inconsistency is found between the two approaches, given the simplifications present in both [4].

2.2 PHYSICS BASED MODELS

A complex interplay between the various branches of micro-instabilities underlying turbulent transport is at the basis of these results. Stability analysis using GS2 indicates that the cases with significant ion heating and very stiff electron temperature profiles are ITG dominated, while in the cases with pure electron heating and weakly stiff electron temperature profiles, the TEM instability starts to dominate the low $\kappa_q\rho_i$ part of the instability spectrum. ETG modes are linearly stable in these plasmas. Detailed predictive modelling of steady-state (T_e, T_i and n_e) and modulation results in both experimental conditions has been reported in [14].

The models tested are: Weiland collisionless and collisional and Bohm-gyroBohm using the transport code JETTO, GLF23 v.1.61 using ASTRA. A comparison of the performance of the models in reproducing modulation data for two shots (Fig.2) with significantly different values of R/L_{Ti} and stiffness levels is shown in Figures 3 and 4 (see [14] for the modelling of steady-state profiles). It is found that experimental results are best reproduced by the Weiland collisional model, which is indeed yielding the same trend of larger electron stiffness for the shot with significant ion heating with respect to the one with dominant electron heating, although the simulated trend is quantitatively less strong than in the experiment.

The complex interplay between electron and ion channels has been theoretically investigated also with the collisionless fluid electrostatic turbulence code TRB [8] . The electron stiffness level in the turbulent simulations has been evaluated by calculating the incremental heat diffusivity, $\chi_{e,hp}= \chi_e +\nabla T_e\delta\chi_e/\delta\nabla T_e$ (Eq.2), whose ratio with the power balance diffusivity can be taken as an estimate of stiffness. This is plotted in figure 5 for various values of P_i/P_e. One can see the increase of electron stiffness when increasing ion heating, although again the trend seems quantitatively weaker than in experiments.

It is clear from this work that, although the physics mechanisms behind temperature profile stiffness are fairly clarified, no quantitative conclusion can yet be drawn regarding profile stiffness in ITER, and no 1st principle model can yet be fully validated for a safe extrapolation. Further experiments are needed in ITER relevant plasmas to evaluate electron and possibly ion stiffness and compare with models.

3. PHYSICS OF INTERNAL TRANSPORT BARRIERS

Although the use of Internal Transport Barriers (ITB) in tokamak plasmas is getting more and more under operational control [15], several key questions on the physics of ITB formation and sustainment still remain unsolved. Amongst these, the type of transition mechanism and turbulence evolution,

the transport properties inside the ITB, the respective roles of the E×B flow shear and magnetic shear and the role of rational surfaces in ITB triggering. In the following sections some recent JET results addressing these issues will be presented.

3.1 ITB TRANSPORT PROPERTIES

Two important questions under debate regarding ITB transport are i) whether the ITB is a region of stiff transport characterized by a threshold R/L_{Tc} larger than in conventional plasmas(case 2 in figure 6) or rather a region below threshold where turbulence is suppressed leading to a loss of stiffness (case 1 in figure 6); ii) whether the improved confinement is limited to a narrow layer or rather extends to the whole core region inside the ITB foot. In order to probe the ITB transport properties, both cold pulses using Ni ablation or shallow pellets and T_e modulation using ICRH in Mode Conversion (^{3}He~12-20%) have been used to generate T_e perturbations travelling across the ITB [16]. While cold pulses have been performed parasitically, T_e modulation has been performed in dedicated experiments using 3.25-3.6T, 2.6-2.9MA plasmas with n_{e0}~3-5$10^{19}$m^{-3} and LH preheat (2-3MW) to achieve deeply reversed magnetic shear (s). The ITB is located in the region of negative s. Up to 18MW of NBI power and 4MW of ICRH power modulated with half depth at 15-45Hz with duty cycle ~60% were applied. The MC power has been localized either at the ITB layer, providing a heat wave generated in the ITB region, or just outside it, providing a heat wave that travels towards the ITB. The ITB is mainly sustained by NBI power, but when the RF is deposited inside the ITB radius, the good localization of RF power using ^{3}He allows to reach outstanding plasma performance, with T_{i0}~24keV, T_{e0}~13keV, n_{e0}~5 10^{19} m^{-3}, at an additional total power level of 15MW. The equivalent Q_{DT} is estimated to be ~0.25 in these discharges [16,17].

Figures 7 and 8 show steady-state profiles of T_e, T_i, n_e, q and profiles of amplitudes (A) and phases (φ) at 1st harmonic of the T_e heat wave obtained by standard FFT techniques. Figure 7 refers to a case in which the MC power was located in the ITB layer; the heat wave is then travelling in two directions away from the ITB. Figure 8 refers to a case in which the MC was located just outside the (weaker) ITB. Note that in this case a fraction of the power is also deposited to electrons in the centre via fast wave Landau damping, so there are two heat waves propagating towards the ITB, one from the centre and one from the outer region.

Both figure 7 and 8 show sharp changes of the heat wave propagation both at the foot and at the top of the high ∇T_e region, providing the answer to question ii), at least for these reverse shear ITBs: the ITB is indeed a narrow layer with low χ_e embedded in a higher χ_e plasma, and not due to a general improvement of confinement in the core region. Regarding question i), FIG.8 shows that the heat wave is strongly damped when meeting the ITB from either side, implying that the ITB is a layer where the perturbative (incremental) diffusivity $\chi_{e,hp}$ (see Eq.2) is very low. Starting from the experimental case in figure 8, using a model of the type of Eq.1, the heat wave propagation has been simulated for both hypotheses, by simply changing the value of κ_c. Figure 9 shows the results. Case 1) corresponds to a situation of complete loss of stiffness due to the plasma having become

fully sub-critical with respect to an increased threshold value. In this case only the second term in Eq.1 survives, χ_e does not depend on ∇T_e the perturbative χ_e coincides with the power balance χ_e and is low, the two heat waves are strongly damped and cannot cross the ITB, the phase exhibits a sharp jump. Case 2) corresponds to a situation where the plasma in the ITB is close to marginality and very stiff: in this case the incremental χ_e is very large, the wave propagates fast inside ITB (small phase change), the amplitudes are not strongly damped so that the two heat waves cross the ITB and get superimposed. One can see that the experiment corresponds to the situation of case 1).

From figure 8, one can also notice that χ_e is not uniform inside the ITB: the slopes of A and φ show that the inner part has lower χ_e, i.e. a stronger stabilization of turbulence. The outer part shows reduced χ_e compared to outside ITB, but still higher than in the inner ITB region. This could correspond to partial stabilization, or to a situation which gets closer to the threshold. In other words the ITB layer gets more fragile in the region near its foot. This observation is in agreement with earlier studies of JET ITBs using cold pulses from the edge[3]. The cold pulse showed a growth when meeting the ITB foot (corresponding to transport re-enhanced in the more fragile outer ITB part) and then a strong damping further inside. The latter result was recently reproduced by turbulence simulations by TRB and CUTIE, as shown in figure 10, and is interpreted as an erosion of the less stabilized part of the ITB by cold pulses due to increased T_e gradient associated with the cold wave. Consistently, no sign of amplification of the heat wave (carrying a decrease in ∇T_e) is observed when it meets the ITB foot.

Attempts to model the modulation results are in progress. Empirical models are in general capable to reproduce the experimental features using a properly shaped χ_e profile. Figure 9(a) gives an example. The situation is more difficult with regard to 1st principle models. Unlike for cold pulses, turbulence simulations are not feasible for modulation at 15Hz due to excessive calculation time. The situation of 1D fluid models is at present not satisfactory already for reproduction of steady-state [18,19],so no comparison with the modulation results was yet possible.

3.2 ITB FORMATION

It is a general observation in JET that the current profile is a key parameter for ITB formation [15,18]. The calculated ExB shear is in most cases too small to trigger the transition [18], although it plays a role later in the discharge due to self-sustainment driven by the increased pressure gradient. The positive effect of a reverse q profile in lowering the ITB triggering power threshold with respect to a monotonic q profile has been demonstrated experimentally [20], as well as the stabilizing effect both for electrons [21,22] and ions [23,24]. The formation of an electron ITB for $s<-0.5$ has been found theoretically using TRB [25] (Figure 11). A strong reduction of ion turbulent transport is also found using GS2 for values $s<-2.5$ [26].

The mechanism of α-stabilisation in ITB formation has not been found to play as an important role in JET as for example in DIII-D [19]. In addition to the role of s, a clear role of low order rational magnetic surfaces in ITB formation has been observed experimentally both for ions and

electrons [27, 28, 18]. In monotonic q profile plasmas, the ITB is triggered at a low order q-rational surface when a higher order q-rational appears at the edge, while for reverse shear plasmas, when the value of minimum q reaches an integer value, the ITB is either formed or (if already existing) strengthened and expanded to the region of the integer q_{min}, possibly leading to the formation of multiple barriers. In the framework of electrostatic turbulence using TRB it was proposed that the evidence in reverse shear plasmas could be explained by turbulence stabilization to the increased gap in the density of main rational surfaces [18]. This explanation has however been recently questioned by [29]. A possible alternative explanation was proposed, based on the idea that the local E×B flow shear can be altered by the presence of an MHD island at the rational surface due to local plasma braking [30]. This mechanism would hold both for monotonic and reverse q profiles. However attempts to find experimental evidence in favour of this type of explanation have had a negative outcome so far. Whilst in monotonic q profile cases a burst of MHD activity is associated to ITB triggering by edge rationals (which could generate inner low order islands by mode coupling), no sign of MHD activity or evidence for strong islands has been observed in reverse shear plasmas. Resolving fine changes in toroidal rotation gradients at ITB triggering has been so far outside the capabilities of the Charge Exchange diagnostic. In addition, an experiment was performed in a monotonic q profile plasma with the aim of reproducing this type of ITB triggering mechanism by external means, i.e by application of a resonant helical magnetic field perturbation usingsaddle coils [30]. Although the conditions of reconnection and formation of an MHD island have been reached, this did not lead to ITB triggering. Theoretical analysis of this result has shown that a local change of ExB flow shear induced by toroidal braking due to an MHD island cannot be easily achieved. In fact at low viscosity the large differential rotation prevents field penetration and braking torque, while at high viscosity the braking region is broadened, inducing a self-similar evolution of toroidal rotation profile which does not lead to a significant modification of its shear (Figure 12). Finally, alternative explanations for the role of q-rationals in ITB formation are suggested by CUTIE simulations via two separate mechanisms [9,31]. The E×B zonal flow is strongly modified locally near q-rational values (by poloidal Maxwell-Lorentz torques in addition to the usual Reynolds stresses) where low m,n MHD can be triggered either by direct instabilities or by “inverse” cascades via the modulational instability [9]. Quite distinct from this is the effect of “dynamo” terms in the induction equation which serve to locally “self-organize” the current profile, leading to regions of small magnetic shear near q-rationals, which are observed to play a stabilizing effect on the underlying micro-turbulence. The two-feed back loops operate on both species. These qualitative observations from CUTIE simulations including “profile-turbulence” interactions remain to be quantified and tailored to JET experimental conditions to provide a fully self-consistent picture of the role of the q-profile in the initiation and maintenance of ITB’s. Further progress on this issue is expected in next JET campaigns where a measurement of the poloidal velocity profile will become available, together with an improved resolution of the toroidal one.

CONCLUSIONS

Heat transport studies at JET have allowed some progress in the understanding of issues like temperature profile stiffness or ITB physics which are crucial for ITER exploitation. The results emphasize the importance of carrying on transport studies in ITER relevant plasmas.

REFERENCES

[1]. Garbet, X., et al., "Physics of transport in tokamaks", accepted for publication in Pl. Phys. Control.Fusion

[2]. Mantsinen, M., et al., "Application of ICRF waves in tokamaks beyond heating", Plasma Phys. Control. Fusion **45** (2003) A445

[3]. Mantica, P., et al., "Perturbative transport experiments in JET low or reverse magnetic shear plasmas", Plasma Phys. Control. Fusion **44** (2002) 2185

[4]. Garbet, X., et al., "Profile stiffness and global confinement", Plasma Phys. Control.Fusion **46** (2004) 1351

[5]. Erba, M., et al., "Development of a non-local model for tokamak heat transport in L-mode, H-mode and transient regimes", Plasma Phys. Control. Fusion **39** (1997) 261

[6]. Weiland, J., "Collective modes in inhomogeneous plasma", Kinetic and Advanced Fluid Theory, IoP Publishing, Bristol and Philadelphia 2000

[7]. Waltz, R.E., et al., "A gyro-Landau-fluid transport model", Phys.Plasmas **4** (1997) 2482

[8]. Garbet, X., et al., "Global simulations of ion turbulence with magnetic shear reversal", Phys. Plasmas **8** (2001) 2793

[9]. Thyagaraja, A., et al., "Mesoscale plasma dynamics, transport barriers and zonal flows: simulations and paradigms", Eur. Journ. Mech B/Fluids/B **23** (2004) 475

[10]. Kotschenreuther, M., et al., "Comparison of initial value and eigenvalue codes for kinetic toroidal plasma instabilities", Comp. Phys. Comm. **88** (1995) 128

[11]. BOURDELLE, C., et al., "Stability analysis of improved confinement discharges: internal transport barriers in Tore Supra and radiative improved mode in TEXTOR", Nucl. Fusion **42** (2002) 892

[12]. Mantica, P., et al., "Transient Heat Transport Studies in JET Conventional and Advanced Tokamak Plasmas ", Fusion energy 2002(Proc.19th IAEA, Lyon, 2002), IAEA, Vienna, EX/P1-04

[13]. Mantica, P., et al.,"Heat wave propagation experiments and modelling at JET:L-mode, H-mode, ITBs", in Control. Fusion and Pl. Physics (Proc.30th Eur. Conf. St.Petersburg),O-3.1A,EPS ECA Vol.27A (2003)

[14]. Mantica, P., et al., "Predictive modelling of T_e modulation experiments in JET L- and H-mode plasmas", in Control. Fusion and Pl. Physics (Proc.31th Eur. Conf. London), P1-153, EPS ECA Vol.28G (2004)

[15]. Challis, C.D., "The Use of ITBs in Tokamak Plasmas", accepted in Plasma Phys. Control. Fusion

[16]. Mantica, P., “Power modulation experiments in JET ITB plasmas”, in Control. Fusion and Pl. Physics (Proc.31th Eur. Conf. London), P1-154, EPS ECA Vol.28G (2004)
[17]. Tuccillio, A., et al., “Development on JET of AT Operations for ITER”, this conf., EX/1-1
[18]. Garbet, X., et al., “Micro-stability and transport modeling of ITBs on JET”, Nucl. Fusion **43** (2003) 975
[19]. Tala, T., et al., “Progress in Transport Modelling of ITB Plasmas in JET”, this conference, TH/P2-9
[20]. Challis, C.D., et al., “Influence of the *q*-profile shape on plasma performance in JET”, Plasma Phys. Control. Fusion **44** (2002) 1031
[21]. Hogeweij, G.M.D., et al., “Electron heated ITBs in JET”, Plasma Phys. Control. Fusion **44** (2002) 1155
[22]. Kirneva, N., et al., “Role of the q profile in electron ITB evolution in JET discharges”, in Control. Fusion and Pl. Physics (Proc.31th Eur. Conf. London), P1-152, EPS ECA Vol.28G (2004)
[23]. Wolf, R.C., “Characterisation of ion heat conduction in JET and ASDEX Upgrade plasmas with and without internal transport barriers”, Plasma Phys. Control. Fusion **45** (2003) 1757
[24]. Crisanti, F., et al., “JET RF Dominated Scenarios and Ion ITB Experiments with No External Momentum Input“, this conference, EX/P2-1
[25]. Baranov, Yu.F., et al., “On the link between q-profile and Internal Transport Barriers”, Plasma Phys. Control. Fusion **46** (2004) 1181
[26]. Budny, R.V., et al., “Micro-turbuelnce, heat and particle fluxes in JET and DIII-D ITB plasmas with highly reversed magnetic shear”, in Control. Fusion and Pl. Physics (Proc.30th Eur. Conf. St.Petersburg), O-3.4A, EPS ECA Vol.27A (2003)
[27]. Joffrin, E., et al.,“MHD ITB triggering in low positive shear scenario in JET”, Nucl.Fusion **42**(2002) 235
[28]. Joffrin, ,E., et al.,“ITB triggering by rational magnetic surfaces in tokamaks“,Nucl.Fusion **43**(2003)1167
[29]. Candy, ,J., et al.,“Smoothness of turbulent transport across a min-q surface”,Phys.Plasmas **11** (2004) 1879
[30]. Lazzaro, E., et al., “Effect of electro-dynamic braking force localized on rational surfaces”, submitted for publication to Plasma Phys. Control. Fusion
[31]. De Baar, M., et al., “Global plasma turbulence simulations of q=3 sawtooth-like events in the RTP tokamak”, submitted to Phys. Rev. Lett. (Oct. 2004) (UKAEA Fusion Report, Culham Sci. Centre, FUS 511).

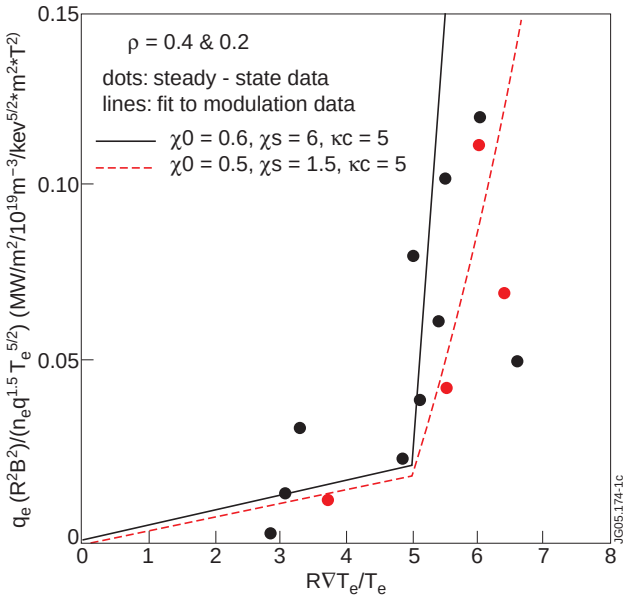

Figure 1: Normalized electron heat flux vs R/L_{Te}. Dots are steady-state data only (ρ=0.2 and 0.4), lines are fits using Eq.(1) to whole profiles of steady-state and modulation data.

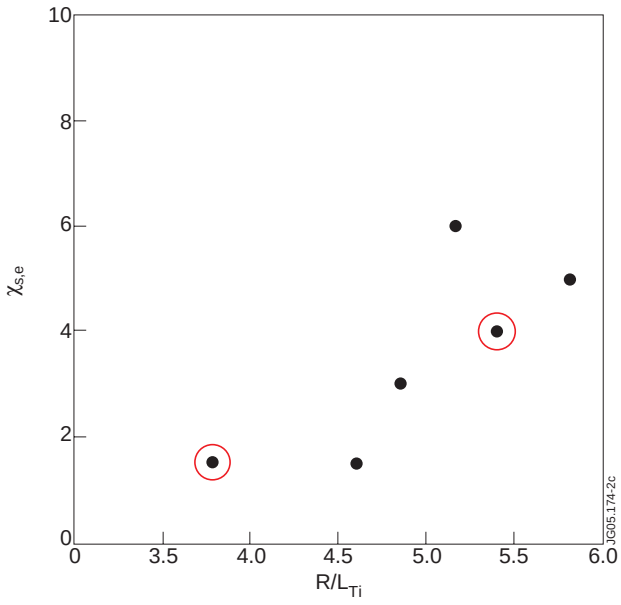

Figure 2: Experimentally determined trend of electron stiffness versus R/L_{Ti}. The two encircled shots are the targets of detailed predictive modelling described in Sect.2.2.

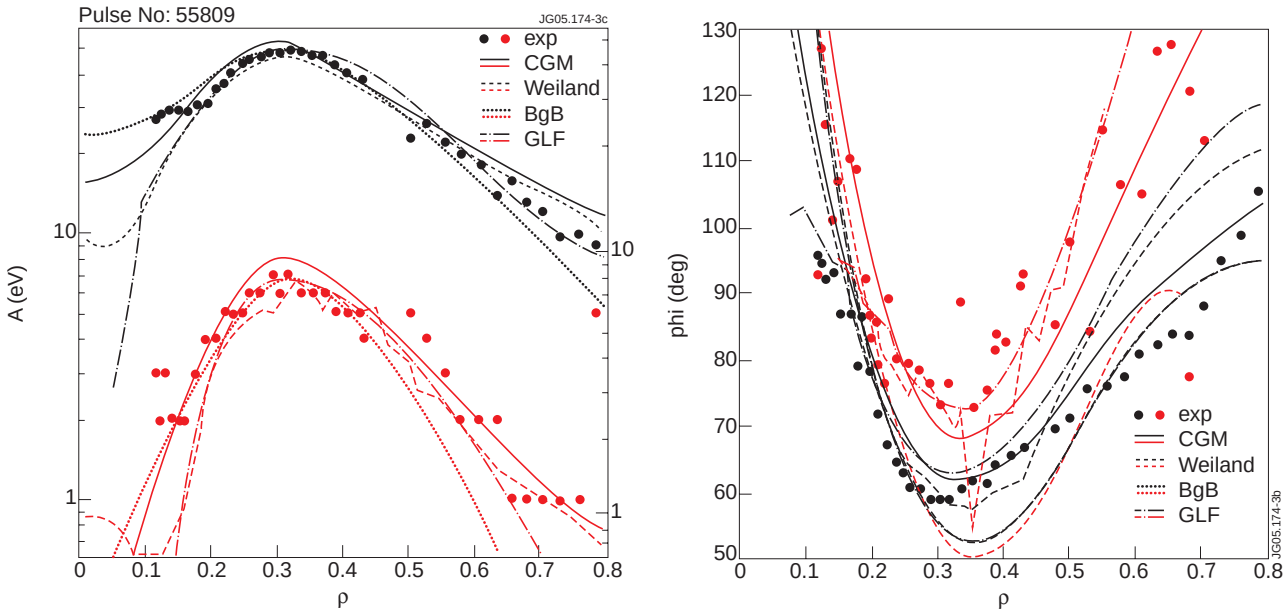

Figure 3: Experimental profiles (dots) of amplitude and phase at 1st (black) and 3rd (red) harmonic for Pulse No: 55809 (large R/L_{Ti}) and simulations (lines) using various models: empirical CGM (solid), Weiland with collisions (small dashed), Bohm-gyroBohm (dotted) and GLF23(long dash).

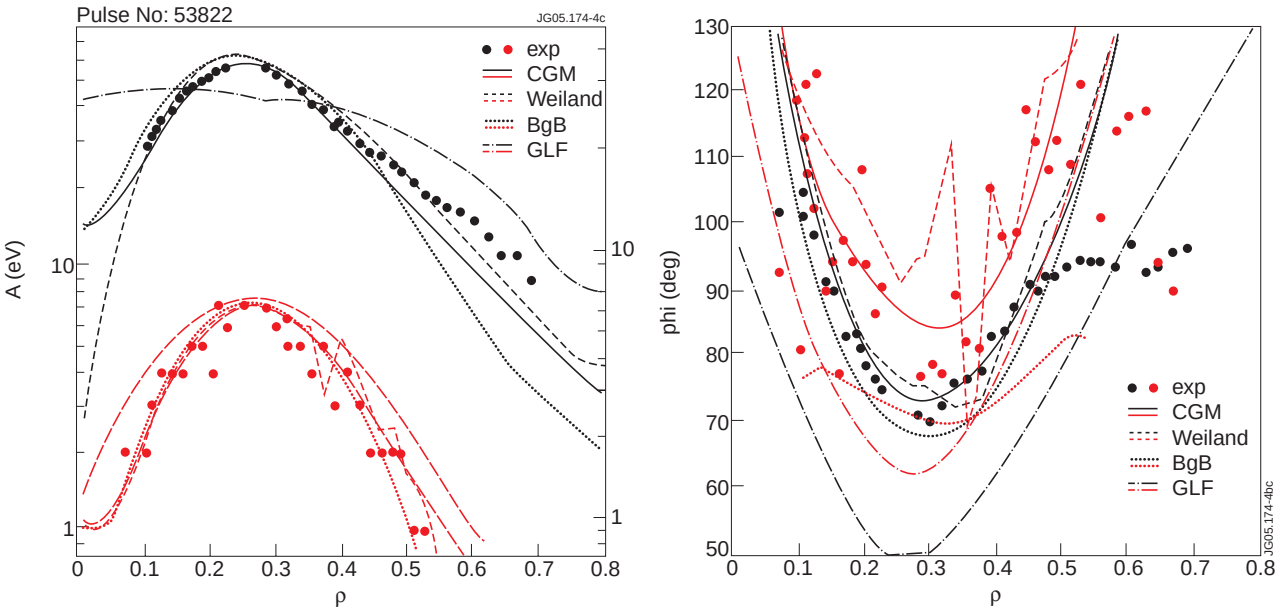

Figure 4: Same as in figure 3 for Pulse No: 53822 (small R/L_{Ti}).

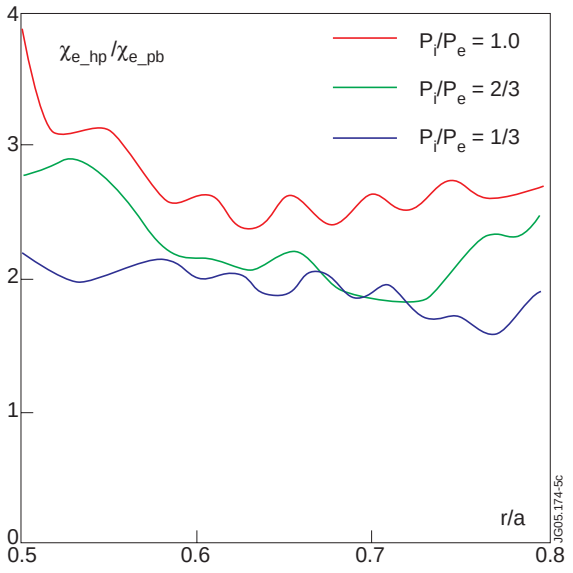

Figure 5: Behaviour of electron stiffness with P_i/P_e estimated from turbulence simulation using TRB

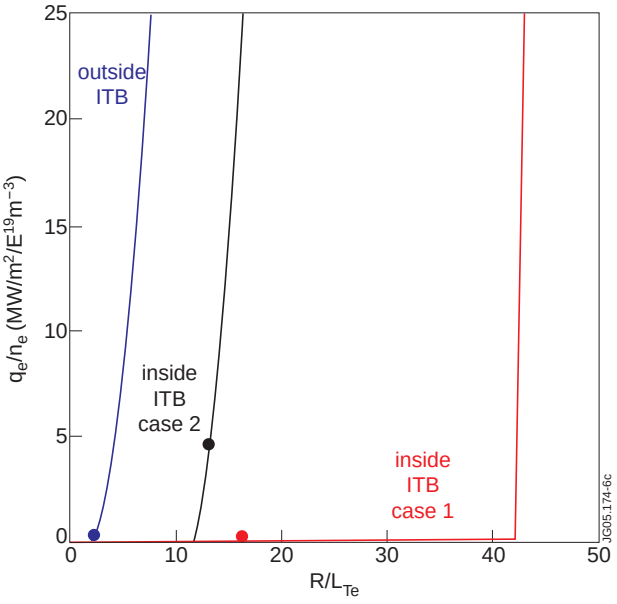

Figure 6: Schematic of the two possible ITB transport pictures discussed in question i)

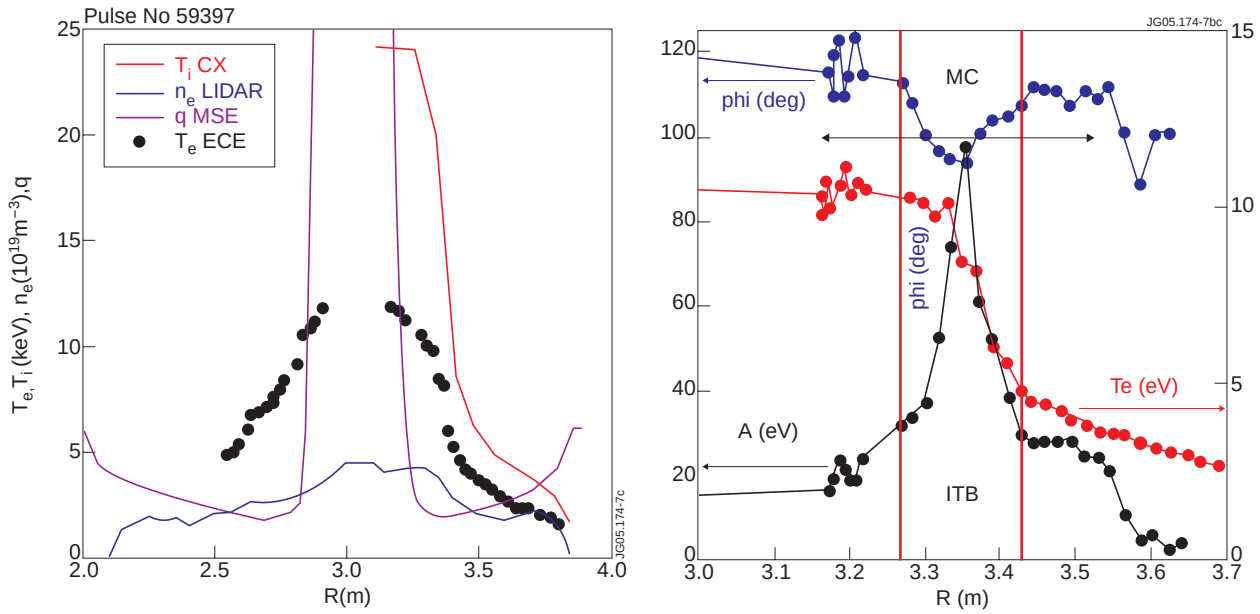

Figure 7: a) Experimental profiles at t=8 s (maximum performance) of T_e, T_i, n_e and q for shot 59397 (3.45T/2.8 MA, ^{3}He~12%, ICRH f=33 MHz). b) profiles of T_e (red), amplitude (black) and phase (blue) at 1st harmonic of the modulation frequency (15 Hz) during the time interval 6.2-6.48 s. Mode converted modulated RF power is applied at the ITB location.

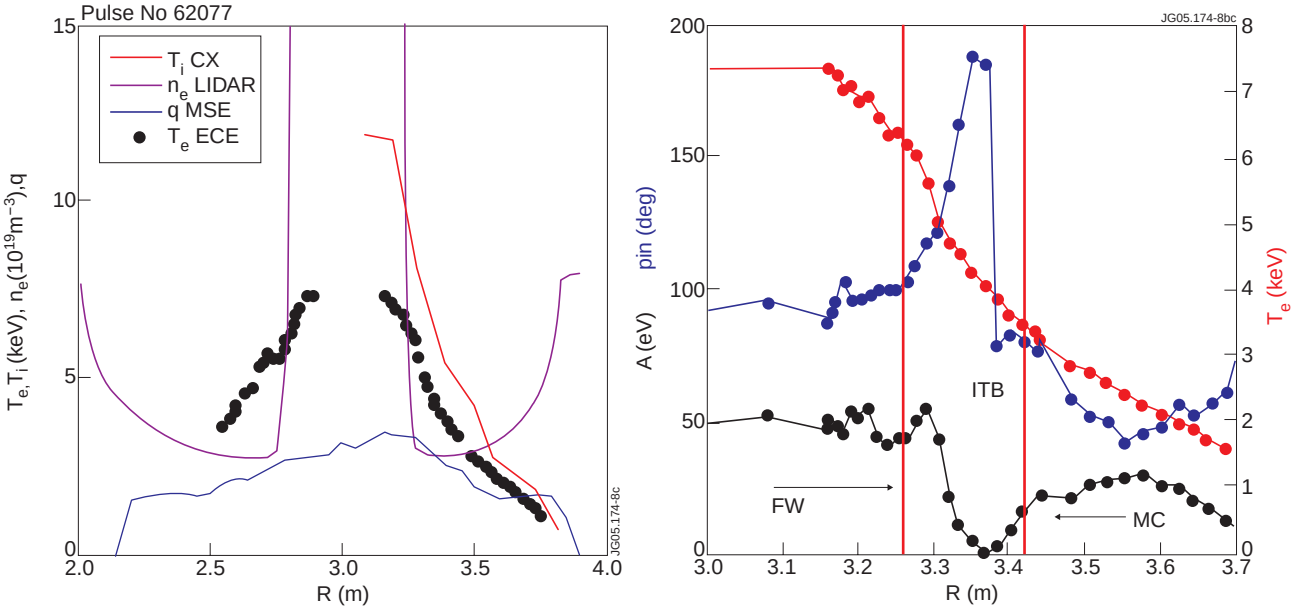

Figure 8: a) Experimental profiles at t=5.5s of T_e, T_i, n_e and q for Pulse No: 62077 (3.25T/2.6 MA, ^{3}He~20%, ICRH f=37MHz). b) profiles of T_e (red), amplitude (black) and phase (blue) at 1st harmonic of the modulation frequency (20Hz) during the time interval 5.5-5.7s. Mode converted modulated RF power is applied outside the ITB location and Fast Wave Landau damping occurs in the core.

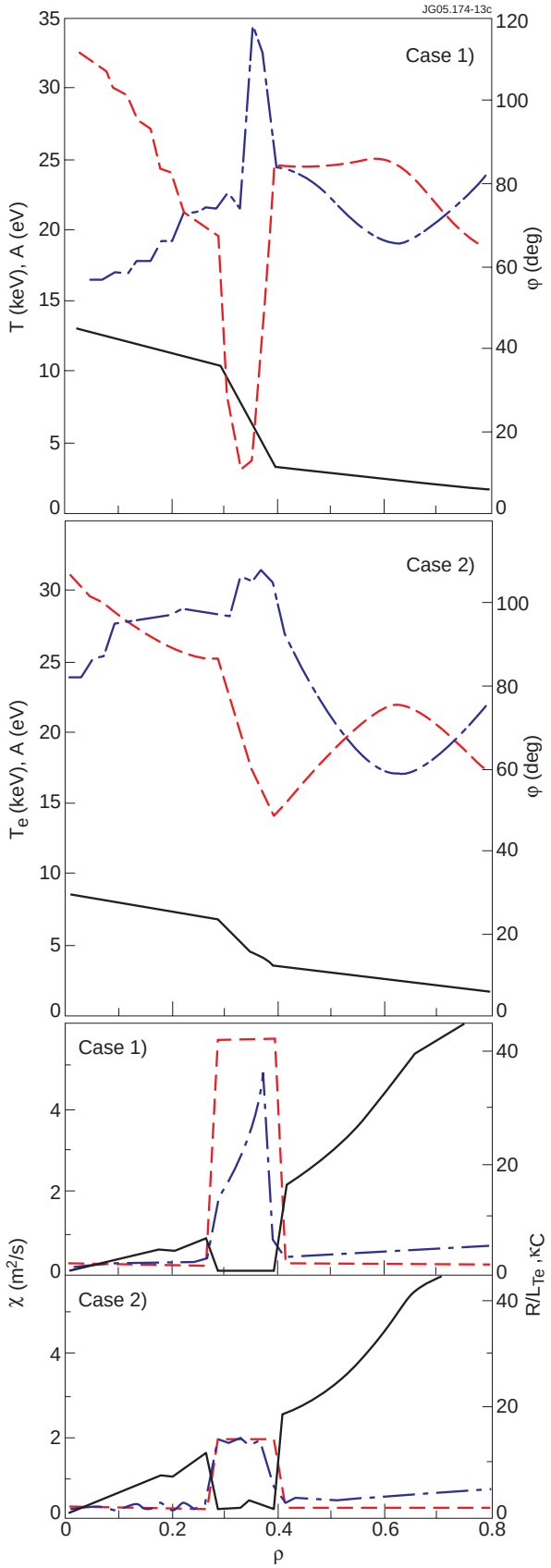

Figure 9(a): simulated T_e (black), A (red) and φ (blue) profiles for case 1 of figure 6 for the experiment in Figure 8. Figure 9(b): same as in Figure 9(a) for case 2 in Figure 6. Figure 9c: profiles of χ_e (black), κ_c (red) and R/L_{Te} (blue) in the two simulations of Figure 9a and b.

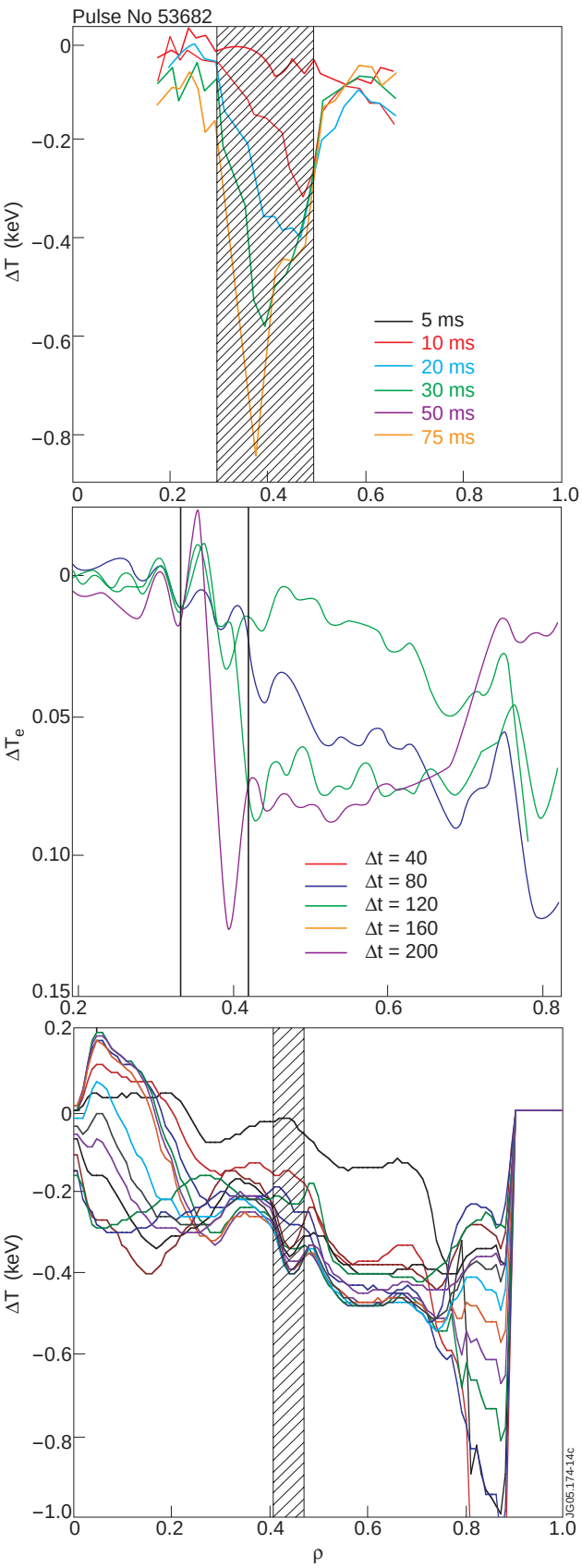

Figure 10: Time evolution of experimental (a) and simulated (b,c) ΔT_e profile following a cold pulse in ITB plasma. (b) with TRB (1 time unit=50μs; 10ms after cold pulse are shown), (c) with CUTIE (15ms after cold pulse are shown).

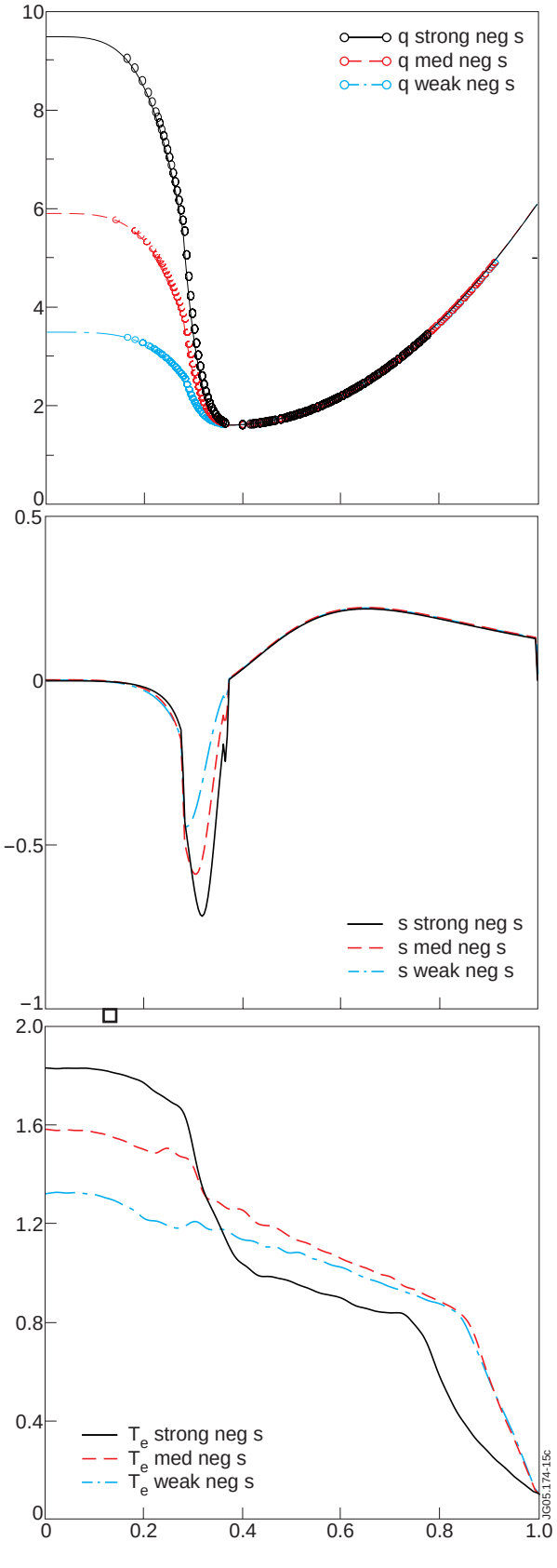

Figure 11: Profiles of safety factor, magnetic shear and electron temperature calculated with TRB.

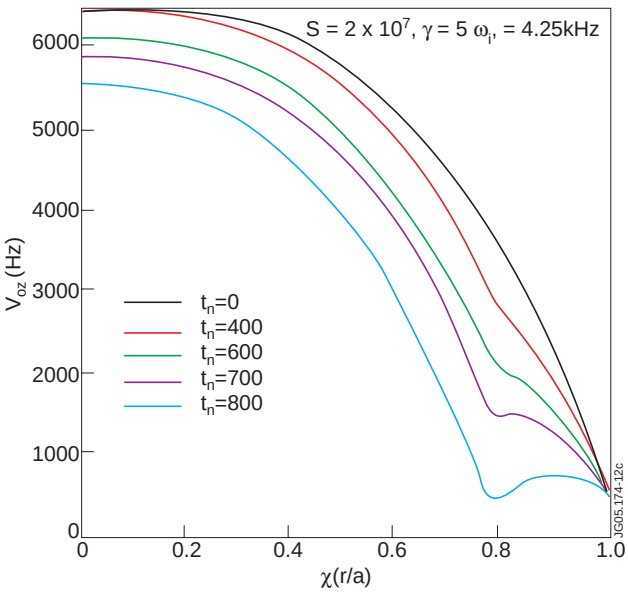

Figure 12: Calculated profile of Vz (r,t) with localized braking force, at high viscosity.